Double-Quantum Spin-Relaxation Limits to Coherence of Near-Surface Nitrogen-Vacancy Centers

B. A. Myers, A. Ariyaratne, and A. C. Bleszynski Jayich

Phys. Rev. Lett. **118**, 197201 — Published 9 May 2017

DOI: 10.1103/PhysRevLett.118.197201

Double-Quantum Spin-Relaxation Limits to Coherence of Near-Surface Nitrogen-Vacancy Centers

B. A. Myers, A. Ariyaratne, A. C. Bleszynski Jayich
Department of Physics, University of California, Santa Barbara, California 93106 USA
(Dated: April 17, 2017)

We probe the relaxation dynamics of the full three-level spin system of near-surface nitrogen-vacancy (NV) centers in diamond to define a T_1 relaxation time that sets the $T_2 \leq 2T_1$ coherence limit of the NV's subset qubit superpositions. We find that double-quantum spin relaxation via electric field noise dominates T_1 of near-surface NVs at low applied magnetic fields. Furthermore, we differentiate $1/f^\alpha$ spectra of electric and magnetic field noise using a novel noise-spectroscopy technique, with broad applications in probing surface-induced decoherence at material interfaces.

Nitrogen-vacancy (NV) centers in diamond excel as room-temperature quantum sensors and quantum bits, where long-lived spin coherence and population are critical to an NV's functionality in these roles. In particular, the coherent control of near-surface NVs has been used to detect few to single electronic spins [1] and nuclear spins [2–4] and to perform nanoscale magnetic resonance imaging [1, 5–7]. The placement of these NVs just nanometers from the diamond surface is vital to strongly couple to external degrees of freedom [8] and achieve nanoscale spatial resolution in imaging [9]. However, our understanding of surface-related noise and its effect on coherence is an incomplete puzzle that remains a grand challenge [10–15] for NV-based sensing. In a broader context, developing a sensor of surface noise on the nanoscale is useful to the study of a variety of quantum technologies, such as trapped ions [16, 17], mechanical resonators [18], and superconducting circuits [19, 20], whose performance is limited by pervasive surface-related decoherence and dissipation.

The NV spin levels that display long coherence reside in the orbital ground state, a three-level spin $S = 1$ system [21]. Any two of the levels may constitute a qubit for coherent quantum sensing and, although the sensor's functionality resides in the coherence of the two-level qubit [22, 23], this functionality is compromised by the coupling of all three levels to the environment. For a two-level system, coherence time T_2 is known to be ultimately limited by spin relaxation time T_1 as $T_2 \leq 2T_1$ [24, 25], and much attention has been paid to this theoretical T_1 limit for NVs [26, 27]. However, for NVs in bulk diamond a saturating $T_2 = 0.53(2)T_1$ has been reported [26], and for shallow NVs, those within ~ 25 nm of the surface, the discrepancy is more striking with $T_2 \lesssim 0.1T_1$ [12, 13]. These prior results suggest a decoherence channel beyond the accounted for spin relaxation and dephasing.

The NV qutrit is rendered a powerful and versatile sensor by the different frequency scales and selection rules of its spin transitions. For precisely the same reasons – the double-edged sword of sensitivity – the NV is also highly susceptible to environmental noise of various origins. The NV has both single-quantum (SQ, $\Delta m_s = \pm 1$) and double-quantum (DQ, $\Delta m_s = \pm 2$) transitions [28] tunable in the MHz to GHz frequency range, as shown in Fig. 1(a). This full capacity of probing noise has not yet been utilized, in particular concerning the direct relaxation rate between the $m_s = \pm 1$ states of the qutrit, which we will refer to as DQ relaxometry. Here, we measure both SQ and DQ relaxation rates of the three-level system and find that shallow NVs exhibit particularly fast DQ relaxation, accounting for decoherence that has not been directly observed before. We then use multipulse dynamical decoupling to show that T_2 of the $m_s = 0, -1$ qubit can exceed a properly defined T_1 at low magnetic fields ($\lesssim 40$ G), where DQ relaxation dominates decoherence. At higher fields, dephasing dominates T_2. Furthermore, because the DQ relaxation channel is a magnetic-dipole-forbidden transition, it can be used to selectively probe electric fields [29] and strain [30–32]. We combine SQ dephasing spectroscopy at high magnetic fields [12, 13, 33] with spectroscopic DQ relaxometry to quantitatively map the spectral character of noise sources responsible for decoherence of near-surface NVs, and this technique enables us to distinguish electric and magnetic contributions to the noise spectrum.

The ground-state spin Hamiltonian [34, 35] of the NV center indicates how magnetic, electric, and strain fields contribute to dephasing and spin relaxation, with the corresponding energy level diagram shown in Fig. 1(a).

$$H_{\mathrm{NV}} = \left(hD_{\mathrm{gs}} + d_\parallel \Pi_\parallel\right) S_z^2 + g\mu_B \mathbf{B}\cdot\mathbf{S} - \frac{d_\perp \Pi_\perp}{2}\left(S_+^2 + S_-^2\right) \quad (1)$$

where $\mathbf{S}$ is the spin-1 operator, h is Planck's constant, $g\mu_B/h = 2.8$ MHz/G is the gyromagnetic ratio, $D_{\mathrm{gs}} = 2.87$ GHz is the crystal-field splitting, $d_\parallel/h = 0.35$ Hz·cm/V and $d_\perp/h = 17$ Hz·cm/V are the components of the NV's electric dipole moment parallel and perpendicular to its symmetry axis [36], and $\Pi_\parallel$ and $\Pi_\perp$ are the corresponding total effective electric field components [34, 35]. $\mathbf{\Pi} = (\mathbf{E} + \boldsymbol{\sigma})$ contains electric field $\mathbf{E}$ and scaled strain $\boldsymbol{\sigma}$ terms. We attribute the $\mathbf{\Pi}$ noise identified in our experimental results with $\mathbf{E}$ electric fields, as discussed in the supplemental sections F.3 and G [37].

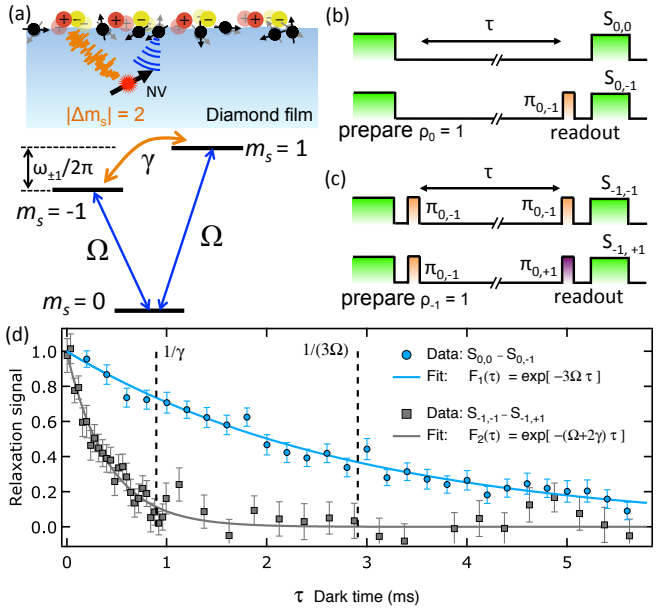

FIG. 1. (a) Surface-noise spectroscopy with the triplet ground state of a shallow NV center. The double-quantum (DQ) relaxation channel (orange, γ) is sensitive to electric field noise, and the single-quantum (SQ) channel (blue, Ω) is sensitive to magnetic field noise. An applied dc magnetic field tunes the DQ transition frequency $\omega_{\pm1}/2\pi$. (b,c) Measurement sequences to extract the relaxation rates Ω and γ. The spin is initialized into population (b) $\rho_0 = 1$ or (c) $\rho_{-1} = 1$ by a green laser pulse and, for $\rho_{-1} = 1$, a microwave $\pi_{0,-1}$ pulse. After a dark time τ, any of the three spin state populations ρ_j can be read out by a choice of $\pi_{0,\pm1}$ pulse before photoluminescence detection, giving signal $S_{i,j}$. (d) Population decay data with three-level relaxation model fits as solid lines.

The spin raising and lowering operators in the last term of Eq. (1) couple the $m_s = \pm1$ states and thus serve as a route for electric noise-induced DQ spin relaxation with a rate γ [Fig. 1(a)]. For the $\{|0\rangle, |-1\rangle\}$ qubit, the $d_{\|}E_{\|}$ term describes electric-field-induced energy shifts [14, 35] that contribute to the dephasing rate $\Gamma_d^{(-10)}$. The second (Zeeman) term accounts for magnetic fields that cause additional dephasing [9, 12, 57] and SQ relaxation [11, 58–61] between $|0\rangle$ and $|\pm1\rangle$ with rates $\Omega_{0,\pm1}$ ($\Omega_{0,+1} = \Omega_{0,-1} \equiv \Omega$, as we verified experimentally, shown in supplementary section C [37]). The energy splitting between the $|\pm1\rangle$ levels, $\hbar\omega_{\pm1} = 2g\mu_B B_z$, is tunable via a dc magnetic field B_z, enabling us to probe the noise spectral density that affects γ [62]. We consider the regime where dc strain, dc electric field, and dc transverse magnetic field are small compared to the applied B_z, so the eigenstates are approximately $\{|0\rangle, |-1\rangle, |+1\rangle\}$ of the S_z operator [35] (see supplementary section H [37]).

For the NV qutrit in Fig. 1(a), the total T_1 relaxation time that limits T_2 of the qubit is built from the relaxation rates between the three $|m_s\rangle$ spin states. However, the most prevalent definition of T_1 in the NV literature [11–13, 27, 33, 58, 63, 64], which we label here $T_1^{(0)} = (3\Omega)^{-1}$, considers only Ω and implicitly assumes $\gamma = 0$. To understand what limits T_2 of the $\{|0\rangle, |-1\rangle\}$ qubit the correct definition should be

$$\frac{1}{T_1} = \frac{1}{T_1^{(0)}} + \gamma = 3\Omega + \gamma. \tag{2}$$

SQ coherence ρ_{-10} initialized between the $|0\rangle$ and $|-1\rangle$ states will decay at a total rate $1/T_2$ due to the sum of pure dephasing $\Gamma_d^{(-10)}$ and spin relaxation rates [65], so that in the zero-dephasing limit $T_2^{\mathrm{SQmax}} = 2T_1 = 2(3\Omega + \gamma)^{-1}$ (see supplementary section D [37]). Hence, to evaluate the revised decoherence limit $T_2 \leq 2T_1$, we first used SQ and DQ relaxometry to extract Ω and γ, and then used dynamical decoupling to reduce $\Gamma_d^{(-10)}$.

The experimental setup consists of a homebuilt, room-temperature confocal microscope with a 532-nm excitation laser and single-photon counters to collect sideband photoluminescence (PL) [66]. A single-crystal diamond film was epitaxially grown using isotopically purified methane (99.99% ^{12}C) to minimize NV decoherence due to ^{13}C nuclear spins [67]. The sample contains NVs at a mean depth of 7 nm, formed via 4-keV nitrogen implantation [10, 68] (see supplementary section A [37]). A microwave stripline was used for coherent $|0\rangle \leftrightarrow |\pm1\rangle$ spin rotations, namely spin inversion $\pi_{0,\pm1}$ pulses [69].

The rates Ω and γ can be experimentally determined by measuring the decay of each diagonal element of the density matrix through pulsed optically detected magnetic resonance [63]. The population dynamics of the $\{|m_s\rangle\}$ are given by three differential equations with the solutions [37, 58, 64]

$$\rho_0(\tau) = \frac{1}{3} + \left(\rho_0(0) - \frac{1}{3}\right) e^{-3\Omega\tau} \tag{3}$$

$$\rho_{\mp1}(\tau) = \frac{1}{3} \mp \frac{1}{2}\Delta\rho(0)\, e^{-(\Omega+2\gamma)\tau} - \frac{1}{2}\left(\rho_0(0) - \frac{1}{3}\right) e^{-3\Omega\tau} \tag{4}$$

where τ is the time between initialization and readout, ρ_{m_s} are the $|m_s\rangle$ state populations, and the initial conditions are $\rho_0(0)$ and $\Delta\rho(0) = [\rho_{+1}(0) - \rho_{-1}(0)]$ (see supplementary section B [37]). We note that a green laser pulse only polarizes the spin to $\rho_0(0) \lesssim 0.80$ [70], but the remaining mixed population only reduces the PL contrast of the measurement.

We performed two sets of experiments using two sets of pulse sequences [Fig. 1(b,c)] that directly probe the spin populations under initial conditions $\rho_i(0) = 1$. The final $\pi_{0,j}$ pulse before PL readout determines which population $\rho_j(\tau)$ is probed, yielding a relaxation signal $S_{i,j}(\tau)$. Figure 1(b) shows a standard method to measure $T_1^{(0)} = (3\Omega)^{-1}$ [63], and applying this sequence to

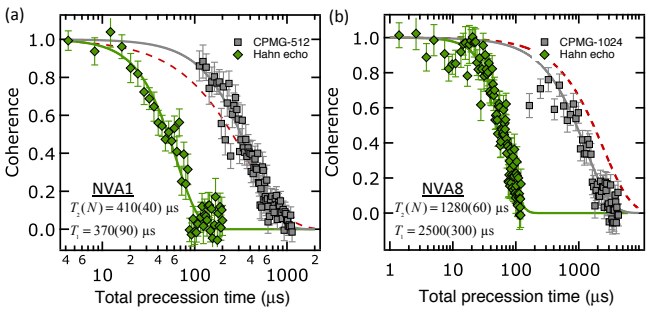

FIG. 2. Enhancement of SQ coherence time using CPMG-N for shallow NVs under conditions of (a) large γ at $\omega_{\pm1}/2\pi = 37.1$ MHz and (b) small γ at $\omega_{\pm1}/2\pi = 1376$ MHz. Data shown are Hahn echo (green diamonds) and CPMG-N (gray squares) where N is the number of π pulses, and solid lines are fits to $\exp\left[-(T/T_2)^n\right]$. Dashed red lines are reference plots of $\exp\left(-T/T_1\right)$ using the measured $T_1 = (3\Omega + \gamma)^{-1}$.

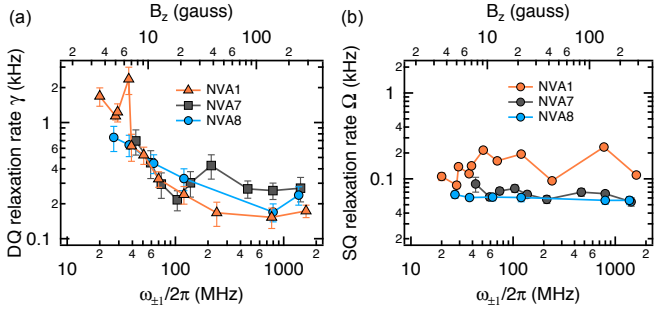

FIG. 3. (a) Measured DQ relaxation rates γ for three shallow NV centers versus DQ frequency splitting $f = \omega_{\pm1}/2\pi$ tuned by applied field B_z. Each symbol type refers to one NV. The $1/f^\alpha$-type dependence is attributed to surface-related electric field noise and saturation at large $\omega_{\pm1}$ is attributed to bulk effects. (b) Measured SQ relaxation rate Ω for the same NVs.

Eqs. (3) and (4) gives a fit function [37]

$$F_1(\tau) = S_{0,0}(\tau) - S_{0,-1}(\tau) = re^{-3\Omega\tau} \qquad (5)$$

where parameter r is PL contrast. The second set of sequences [Fig. 1(c)] initialize $\Delta\rho(0) \neq 0$ and measure $\rho_{\mp1}(\tau)$, and data is fit to [37]

$$F_2(\tau) = S_{-1,-1}(\tau) - S_{-1,+1}(\tau) = re^{-(\Omega+2\gamma)\tau}. \qquad (6)$$

Figure 1(d) shows data for a shallow NV, labeled A1, taken at 6.6 G and fitted to Eqs. (5) (blue circles data) and (6) (gray squares data), revealing a slow SQ rate $\Omega = 0.115(4)$ kHz and faster DQ rate $\gamma = 1.11(5)$ kHz. Hence the traditional relaxation time $T_1^{(0)} = 2.90(3)$ ms overestimates by 4× the full $T_1 = 0.69(7)$ ms from Eq. (2), due to significant DQ relaxation.

The complete T_1 enables evaluation of the limit $T_2 \leq 2T_1$, for which we used a CPMG pulse sequence to dynamically decouple the NV from its environment, leading to a reduced pure dephasing rate $\Gamma_d^{(-10)}$. Figure 2 shows Hahn echo and CPMG-N measurements for two shallow NVs, where N is the number of π_y pulses [71]. The coherence time $T_2 = T_2(N)$ is extracted from a stretched-exponential fit $\exp\left[-(T/T_2)^n\right]$ to data $C(T)$, where $C(T)$ is phase coherence mapped onto spin population after a total precession time T. Figure 2(a) shows that for sufficiently large $N = 512$, and at $\omega_{\pm1}/2\pi = 37.1$ MHz, T_2 saturates at $1.2(3)T_1$, in clear contrast to the incomplete comparison $T_2 = 0.14(1)T_1^{(0)}$ (additional data in supplementary Table II and section E [37]). At a much larger $\omega_{\pm1}/2\pi = 1376$ MHz [Fig. 2(b)], $T_2(N = 1024)$ saturates at only $0.52(7)T_1$, while T_2 and T_1 both increase. The explanation for these changes at higher $\omega_{\pm1}$ lies in the frequency dependence of γ, as we discuss next.

Figure 3(a) shows a strong dependence of γ on frequency $f = \omega_{\pm1}/2\pi$ for shallow NVs, with two implications: 1) T_1 greatly decreases at lower magnetic fields, in contrast to $T_1^{(0)}$, and 2) double-quantum relaxation spectroscopy gives new insights about noise sources affecting γ. As B_z tunes $\omega_{\pm1}/2\pi$ from 1612 MHz to 20 MHz, γ increases by up to an order of magnitude, showing a $1/f^\alpha + \gamma_\infty$ type of dependence with $\alpha = 1 - 2$. We observe the $1/f^\alpha$ part only for shallow NVs, those less than about 25 nm from the surface (see [12] and supplemental section E.2 [37]), and thus we identify its origin as surface-related electric field noise [37]. We attribute γ_∞ relaxation to bulk effects [37, 72]. In contrast to γ, we show in Fig. 3(b) that Ω is independent of magnetic field over the studied range of $B_z \approx 4 - 290$ G [63]. The ratio γ/Ω demonstrates that the DQ relaxation contributes substantially to the total decoherence rate; $\gamma/\Omega \gg 1$ at low B_z and $\gamma/\Omega \gtrsim 1$ even at higher B_z. The suppression of shallow-NV decoherence via the DQ channel at large $\omega_{\pm1}$ gives a practical reason for magnetometry experiments to operate at $B_z > 100$ G, and it also explains our observation in Fig. 2: relaxation slows down as $\omega_{\pm1}$ increases, and dephasing takes over as the dominant decoherence channel. $\Gamma_d^{(-10)}$ cannot be eliminated completely because experimental limitations to π pulse duration and spacing restrict the maximum CPMG filter frequency $f_{\max}$ to a few MHz. The noise spectrum that causes dephasing, although decaying in frequency, has a finite value at $f_{\max}$, which explains why we do not reach $T_2 = 2T_1$ even for large γ (short T_1). The T_2/T_1 ratio is reduced at small γ because higher N is required to make $\Gamma_d^{(-10)} \ll 1/T_1$. Future CPMG experiments at higher values of $f_{\max}$ could probe the effects of higher frequency noise sources on pure dephasing.

Finally, we identify the spectra of surface electric and magnetic field noise over a broad frequency range by employing a combination of SQ dephasing spectroscopy [13, 14, 25, 33, 73, 74] and DQ relaxometry. These complementary techniques are summarized in Table I and detailed in supplementary section F [37]. SQ dephasing spectra $S_{\rm cpmg}(f)$ and DQ relaxation spectra $S_\gamma(f)$,

	DQ relaxation spectroscopy	SQ dephasing spectroscopy
Measurement	Relaxation between $m_s = \pm 1$ populations	CPMG multipulse on NV superposition
Filter frequency tuning	Applied B_z: $\omega_{\pm 1}/2\pi \approx 2g\mu_B B_z/h$	Number N and spacing T/N of π pulses
Primary noise probed	$\Pi_\perp$ at f = [10 MHz - few GHz]	B_z and $\Pi_\parallel$ at f = [10 kHz - few MHz]
Coupling power [Hz^2/Hz]	$S(\omega_{\pm 1}) = \gamma$	$S(\omega = \pi N/T) \approx -\pi \ln C(T)/T$
Assumption for validity	$g\mu_B B_z/h \gg \Pi_\perp d_\perp/h \implies$ eigenstates $\lvert m_s\rangle$	$B_z \gtrsim 100$ G $\implies$ small γ: $T_2 \ll T_1$

TABLE I. Comparison and complementarity of relaxation and dephasing for classical-noise spectroscopy with NV centers.

in units of coupling power Hz^2/Hz, were generated from measurements like those presented in Figs. 2 and 3, respectively. The two spectral densities each have distinct noise origins (Table I), and hence "coupling power" has different meanings for dephasing and relaxation. Therefore, to directly compare $S_{\text{cpmg}}(f)$ and $S_\gamma(f)$ we scale each from a coupling rate to a shared effective transverse electric field noise power spectrum:

$$S_{E_\perp}^{\text{cpmg}}(f) = 2\frac{S_{\text{cpmg}}(f)}{d_\parallel^2/h^2}; S_{E_\perp}^{\gamma}(f) = \frac{S_\gamma(f)}{d_\perp^2/h^2}. \quad (7)$$

Equation 7 enables us to jointly model the dephasing and relaxation spectra (see supplementary section F.3 [37]), and the results are shown in Fig. 4, where the left axis of each plot is coupling power and the right axis is transverse electric noise power. To fit the $S_{E_\perp}^{\text{cpmg}}(f)$ and $S_{E_\perp}^{\gamma}(f)$ data we assume a stationary Gauss-Markov process for electric and magnetic field sources [74]. A double-Lorentzian is the sum of two such processes with different total noise power and frequency cutoffs. The fit results show that the electric Lorentzian (blue dash-dot line) has a lower cutoff frequency than the magnetic noise (red dashed line): for NVA1 $\tau_e \approx 1\ \mu$s and $\tau_m \approx 100$ ns. For NVA8, $\tau_m \approx 400$ ns and its electric noise curve actually fits best as $1/f^\alpha$ with $\alpha = 1.5$. This $\alpha < 2$ frequency dependence can be constructed from a sum of many discrete Lorentzians with a range of correlation times, as postulated for noise from charge traps [75] or fluctuating electric dipoles [16].

Our spectroscopy results help tie together prior work [11–14] on decoherence of near-surface NVs, which primarily focused on magnetic noise. Kim *et. al.* [14] gave evidence for shallow-NV dephasing via $1/f$-like $E_\parallel$ electric field noise by showing that 1) dephasing noise is reduced when a high-dielectric-constant liquid is placed on the diamond surface, and 2) coherences of SQ and DQ qubits exhibit a ratio that cannot be explained by purely magnetic noise. Our addition of DQ relaxometry to the surface-noise-spectroscopy toolbox enables us to differentiate magnetic and electric noise sources, and importantly, our two-bath model identifies the lower-frequency noise component to be electric, in contrast to previous experiments [12, 13]. Together with previous depth-resolved work that identified a $1/d^{3.6(4)}$ dependence of $S_{\text{cpmg}}(f)$ [12, 13], we suggest that electric field noise from fluctuating electric dipole moments, such as modeled on

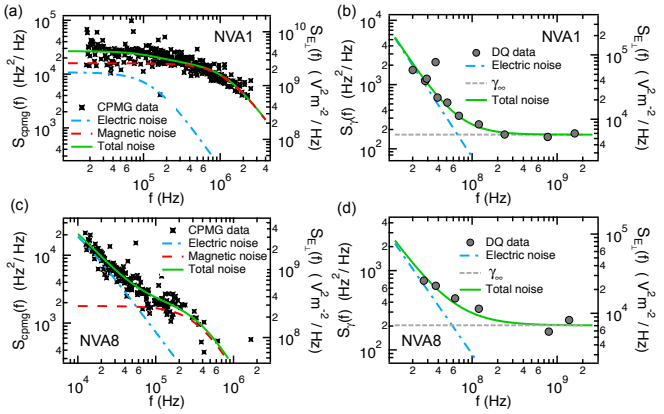

FIG. 4. Measured noise spectra in terms of coupling power (Hz^2/Hz) and transverse electric field power (V^{2}m^{-2}/Hz) for shallow NVs A1 (a,b) and A8 (c,d) using dephasing spectroscopy (left plots) and DQ relaxation spectroscopy (right plots). Each NV data set is jointly fit to a noise model (green solid line) of three parts: $1/f^\alpha$-like electric fields (blue dash-dot line), magnetic fields (red dashed line), and a minimum relaxation rate γ_∞ due to bulk effects (horizontal dashed line).

metal electrodes in ion traps [16, 17], could explain the observed results. Furthermore, we note that the magnitudes of our observed $S_{E_\perp}(f)$ are quantitatively consistent with those reported in experiments on ion-trap heating rates (see [76] and supplementary section G.1 [37]). Looking forward, the DQ relaxation technique can be readily combined with single-NV scanning probe microscopy [59, 77, 78] to investigate the microscopic origins of noise from various surfaces.

In conclusion, we have highlighted the importance of considering the coupling between all three levels of the NV ground state for understanding NV decoherence, especially for near-surface NVs. We find the double-quantum (DQ) spin relaxation rate γ to be a major, and even dominant, contributor to the limit of qubit coherence time T_2. We have also used shallow NVs to perform combined dephasing and DQ relaxation spectroscopies of diamond surfaces and furthermore demonstrated a method to distinguish electric and magnetic field noise. To gain more insight into diamond-surface-related electric field noise, several experiments could be revisited with γ measured in tandem with T_2. Since γ should be even larger for ultra-shallow NVs at depths of

2-5 nanometers [2, 79, 80], one could sensitively probe the effects of, for example, annealing and thermal oxidation [15, 81], plasma etching [82, 83], surface termination [84–86], chemical treatments [80], temperature [11, 63], photoinduced space charge [87], and variations in the work function [88]. The DQ relaxometry technique we have presented will also be a useful asset for understanding the coupling of general spin $S > 1/2$ solid-state defects to interfaces in hybrid systems.

The authors thank K. Lee, D. Rugar, and J. Mamin for helpful discussions. P. Ovartchaiyapong performed the electron beam lithography for nanopillars and provided helpful knowledge on diamond fabrication. The authors thank D. D. Awschalom and K. Ohno for providing diamond growth equipment and training. This work was supported by the DARPA QuASAR program and the AFOSR YIP. B.A.M. acknowledges support from the Department of Defense (NDSEG) and the IBM Ph.D. Fellowship Program.

[1] M. S. Grinolds, S. Hong, P. Maletinsky, L. Luan, M. D. Lukin, R. L. Walsworth, and A. Yacoby, Nat Phys **9**, 215 (2013).
[2] M. Loretz, S. Pezzagna, J. Meijer, and C. L. Degen, Applied Physics Letters **104**, 033102 (2014).
[3] A. O. Sushkov, I. Lovchinsky, N. Chisholm, R. L. Walsworth, H. Park, and M. D. Lukin, Phys. Rev. Lett. **113**, 197601 (2014).
[4] C. Müller, X. Kong, J. M. Cai, K. Melentijević, A. Stacey, M. Markham, D. Twitchen, J. Isoya, S. Pezzagna, J. Meijer, J. F. Du, M. B. Plenio, B. Naydenov, L. P. McGuinness, and F. Jelezko, Nat Commun **5**, 4703 (2014).
[5] M. S. Grinolds, M. Warner, K. De Greve, Y. Dovzhenko, L. Thiel, R. L. Walsworth, S. Hong, P. Maletinsky, and A. Yacoby, Nat Nano **9**, 279 (2014).
[6] D. Rugar, H. J. Mamin, M. H. Sherwood, M. Kim, C. T. Rettner, K. Ohno, and D. D. Awschalom, Nat Nano **10**, 120 (2015).
[7] T. Häberle, D. Schmid-Lorch, F. Reinhard, and J. Wrachtrup, Nat Nano **10**, 125 (2015).
[8] J. Cai, A. Retzker, F. Jelezko, and M. B. Plenio, Nat Phys **9**, 168 (2013).
[9] J. M. Taylor, P. Cappellaro, L. Childress, L. Jiang, D. Budker, P. R. Hemmer, A. Yacoby, R. Walsworth, and M. D. Lukin, Nat Phys **4**, 810 (2008).
[10] B. K. Ofori-Okai, S. Pezzagna, K. Chang, M. Loretz, R. Schirhagl, Y. Tao, B. A. Moores, K. Groot-Berning, J. Meijer, and C. L. Degen, Phys. Rev. B **86**, 081406 (2012).
[11] T. Rosskopf, A. Dussaux, K. Ohashi, M. Loretz, R. Schirhagl, H. Watanabe, S. Shikata, K. M. Itoh, and C. L. Degen, Phys. Rev. Lett. **112**, 147602 (2014).
[12] B. A. Myers, A. Das, M. C. Dartiailh, K. Ohno, D. D. Awschalom, and A. C. Bleszynski Jayich, Phys. Rev. Lett. **113**, 027602 (2014).
[13] Y. Romach, C. Müller, T. Unden, L. J. Rogers, T. Isoda, K. M. Itoh, M. Markham, A. Stacey, J. Meijer, S. Pezzagna, B. Naydenov, L. P. McGuinness, N. Bar-Gill, and F. Jelezko, Phys. Rev. Lett. **114**, 017601 (2015).
[14] M. Kim, H. J. Mamin, M. H. Sherwood, K. Ohno, D. D. Awschalom, and D. Rugar, Phys. Rev. Lett. **115**, 087602 (2015).
[15] J. Wang, W. Zhang, J. Zhang, J. You, Y. Li, G. Guo, F. Feng, X. Song, L. Lou, W. Zhu, and G. Wang, Nanoscale **8**, 5780 (2016).
[16] A. Safavi-Naini, P. Rabl, P. F. Weck, and H. R. Sadeghpour, Phys. Rev. A **84**, 023412 (2011).
[17] D. Hite, Y. Colombe, A. Wilson, D. Allcock, D. Leibfried, D. Wineland, and D. Pappas, MRS Bulletin **38**, 826 (2013).
[18] B. C. Stipe, H. J. Mamin, T. D. Stowe, T. W. Kenny, and D. Rugar, Phys. Rev. Lett. **87**, 096801 (2001).
[19] F. C. Wellstood, C. Urbina, and J. Clarke, Applied Physics Letters **50**, 772 (1987).
[20] R. de Sousa, Phys. Rev. B **76**, 245306 (2007).
[21] M. W. Doherty, N. B. Manson, P. Delaney, F. Jelezko, J. Wrachtrup, and L. C. Hollenberg, Physics Reports **528**, 1 (2013).
[22] J. R. Maze, P. L. Stanwix, J. S. Hodges, S. Hong, J. M. Taylor, P. Cappellaro, L. Jiang, M. V. G. Dutt, E. Togan, A. S. Zibrov, A. Yacoby, R. L. Walsworth, and M. D. Lukin, Nature **455**, 644 (2008).
[23] L. Rondin, J.-P. Tetienne, T. Hingant, J.-F. Roch, P. Maletinsky, and V. Jacques, Reports on Progress in Physics **77**, 056503 (2014).
[24] C. Slichter, *Principles of Magnetic Resonance*, 3rd ed. (Springer-Verlag Berlin Heidelberg, 1990).
[25] J. Bylander, S. Gustavsson, F. Yan, F. Yoshihara, K. Harrabi, G. Fitch, D. G. Cory, Y. Nakamura, J.-S. Tsai, and W. D. Oliver, Nat Phys **7**, 565 (2011).
[26] N. Bar-Gill, L. M. Pham, A. Jarmola, D. Budker, and R. L. Walsworth, Nat Commun **4**, 1743 (2013).
[27] H. S. Knowles, D. M. Kara, and M. Atatüre, Nat Mater **13**, 21 (2014).
[28] N. B. Manson, X.-F. He, and P. T. H. Fisk, Opt. Lett. **15**, 1094 (1990).
[29] P. V. Klimov, A. L. Falk, B. B. Buckley, and D. D. Awschalom, Phys. Rev. Lett. **112**, 087601 (2014).
[30] E. R. MacQuarrie, T. A. Gosavi, N. R. Jungwirth, S. A. Bhave, and G. D. Fuchs, Phys. Rev. Lett. **111**, 227602 (2013).
[31] A. Barfuss, J. Teissier, E. Neu, A. Nunnenkamp, and P. Maletinsky, Nat Phys **11**, 820 (2015).
[32] P. Ovartchaiyapong, K. W. Lee, B. A. Myers, and A. C. Bleszynski Jayich, Nat Commun **5**, 4429 (2014).
[33] N. Bar-Gill, L. M. Pham, C. Belthangady, D. Le Sage, P. Cappellaro, J. R. Maze, M. D. Lukin, A. Yacoby, and R. Walsworth, Nat Commun **3**, 858 (2012).
[34] M. W. Doherty, F. Dolde, H. Fedder, F. Jelezko, J. Wrachtrup, N. B. Manson, and L. C. L. Hollenberg, Phys. Rev. B **85**, 205203 (2012).
[35] F. Dolde, H. Fedder, M. W. Doherty, T. Nobauer, F. Rempp, G. Balasubramanian, T. Wolf, F. Reinhard, L. C. L. Hollenberg, F. Jelezko, and J. Wrachtrup, Nat Phys **7**, 459 (2011).
[36] E. van Oort and M. Glasbeek, Chemical Physics Letters **168**, 529 (1990).
[37] See supplemental material at url for diamond sample information, measurement methods, spectroscopy analysis, and derivation of electric noise models, which includes Refs. [38-56].
[38] B. J. M. Hausmann, T. M. Babinec, J. T. Choy, J. S.

Hodges, S. Hong, I. Bulu, A. Yacoby, M. D. Lukin, and M. Lončar, New Journal of Physics **13**, 045004 (2011).
[39] S. A. Momenzadeh, R. J. Stöhr, F. F. de Oliveira, A. Brunner, A. Denisenko, S. Yang, F. Reinhard, and J. Wrachtrup, Nano Letters **15**, 165 (2015).
[40] S. Kolkowitz, A. Safira, A. A. High, R. C. Devlin, S. Choi, Q. P. Unterreithmeier, D. Patterson, A. S. Zibrov, V. E. Manucharyan, H. Park, and M. D. Lukin, Science **347**, 1129 (2015).
[41] K. Ohno, F. J. Heremans, L. C. Bassett, B. A. Myers, D. M. Toyli, A. C. Bleszynski Jayich, C. J. Palmstrøm, and D. D. Awschalom, Applied Physics Letters **101**, 082413 (2012), http://dx.doi.org/10.1063/1.4748280.
[42] H. J. Mamin, M. H. Sherwood, M. Kim, C. T. Rettner, K. Ohno, D. D. Awschalom, and D. Rugar, Phys. Rev. Lett. **113**, 030803 (2014).
[43] P. Huang, X. Kong, N. Zhao, F. Shi, P. Wang, X. Rong, R.-B. Liu, and J. Du, Nat Commun **2**, 570 (2011).
[44] P. Jamonneau, M. Lesik, J. P. Tetienne, I. Alvizu, L. Mayer, A. Dréau, S. Kosen, J.-F. Roch, S. Pezzagna, J. Meijer, T. Teraji, Y. Kubo, P. Bertet, J. R. Maze, and V. Jacques, Phys. Rev. B **93**, 024305 (2016).
[45] E. R. MacQuarrie, T. A. Gosavi, S. A. Bhave, and G. D. Fuchs, Phys. Rev. B **92**, 224419 (2015).
[46] G. E. Uhlenbeck and L. S. Ornstein, Phys. Rev. **36**, 823 (1930).
[47] N. Manson and J. Harrison, Diamond and Related Materials **14**, 1705 (2005).
[48] B. Grotz, M. V. Hauf, M. Dankerl, B. Naydenov, S. Pezzagna, J. Meijer, F. Jelezko, J. Wrachtrup, M. Stutzmann, F. Reinhard, and J. A. Garrido, Nat Commun **3**, 729 (2012).
[49] I. Talukdar, D. J. Gorman, N. Daniilidis, P. Schindler, S. Ebadi, H. Kaufmann, T. Zhang, and H. Häffner, Phys. Rev. A **93**, 043415 (2016).
[50] R. J. Epstein, S. Seidelin, D. Leibfried, J. H. Wesenberg, J. J. Bollinger, J. M. Amini, R. B. Blakestad, J. Britton, J. P. Home, W. M. Itano, J. D. Jost, E. Knill, C. Langer, R. Ozeri, N. Shiga, and D. J. Wineland, Phys. Rev. A **76**, 033411 (2007).
[51] D. A. Hite, Y. Colombe, A. C. Wilson, K. R. Brown, U. Warring, R. Jördens, J. D. Jost, K. S. McKay, D. P. Pappas, D. Leibfried, and D. J. Wineland, Phys. Rev. Lett. **109**, 103001 (2012).
[52] H. Lüth, "Space-charge layers at semiconductor interfaces," in *Solid Surfaces, Interfaces and Thin Films* (Springer Berlin Heidelberg, Berlin, Heidelberg, 2010) pp. 323–376.
[53] K. W. Lee, D. Lee, P. Ovartchaiyapong, J. Minguzzi, J. R. Maze, and A. C. Bleszynski Jayich, Phys. Rev. Applied **2**, 034005 (2016).
[54] D. R. Alfonso, D. A. Drabold, and S. E. Ulloa, Phys. Rev. B **51**, 1989 (1995).
[55] K. Fang, V. M. Acosta, C. Santori, Z. Huang, K. M. Itoh, H. Watanabe, S. Shikata, and R. G. Beausoleil, Phys. Rev. Lett. **110**, 130802 (2013).
[56] C. S. Shin, M. C. Butler, H.-J. Wang, C. E. Avalos, S. J. Seltzer, R.-B. Liu, A. Pines, and V. S. Bajaj, Phys. Rev. B **89**, 205202 (2014).
[57] G. de Lange, Z. H. Wang, D. Ristè, V. V. Dobrovitski, and R. Hanson, Science **330**, 60 (2010).
[58] J.-P. Tetienne, T. Hingant, L. Rondin, A. Cavaillès, L. Mayer, G. Dantelle, T. Gacoin, J. Wrachtrup, J.-F. Roch, and V. Jacques, Phys. Rev. B **87**, 235436 (2013).
[59] M. Pelliccione, B. A. Myers, L. M. A. Pascal, A. Das, and A. C. Bleszynski Jayich, Phys. Rev. Applied **2**, 054014 (2014).
[60] T. van der Sar, F. Casola, R. L. Walsworth, and A. Yacoby, Nat Commun **6**, 7886 (2015).
[61] L. T. Hall, P. Kehayias, D. A. Simpson, A. Jarmola, A. Stacey, D. Budker, and L. C. L. Hollenberg, Nat Commun **7**, 10211 (2016).
[62] R. J. Schoelkopf, A. A. Clerk, S. M. Girvin, K. W. Lehnert, and M. H. Devoret, "Quantum noise in mesoscopic physics," (Springer Netherlands, Dordrecht, 2003) Chap. Qubits as Spectrometers of Quantum Noise, pp. 175–203.
[63] A. Jarmola, V. M. Acosta, K. Jensen, S. Chemerisov, and D. Budker, Phys. Rev. Lett. **108**, 197601 (2012).
[64] S. Steinert, F. Ziem, L. T. Hall, A. Zappe, M. Schweikert, N. Götz, A. Aird, G. Balasubramanian, L. Hollenberg, and J. Wrachtrup, Nat Commun **4**, 1607 (2013).
[65] S. G. Schirmer and A. I. Solomon, Phys. Rev. A **70**, 022107 (2004).
[66] A. Gruber, A. Dräbenstedt, C. Tietz, L. Fleury, J. Wrachtrup, and C. v. Borczyskowski, Science **276**, 2012 (1997).
[67] G. Balasubramanian, P. Neumann, D. Twitchen, M. Markham, R. Kolesov, N. Mizuochi, J. Isoya, J. Achard, J. Beck, J. Tissler, V. Jacques, P. R. Hemmer, F. Jelezko, and J. Wrachtrup, Nat Mater **8**, 383 (2009).
[68] J. R. Rabeau, P. Reichart, G. Tamanyan, D. N. Jamieson, S. Prawer, F. Jelezko, T. Gaebel, I. Popa, M. Domhan, and J. Wrachtrup, Applied Physics Letters **88**, 023113 (2006), http://dx.doi.org/10.1063/1.2158700.
[69] F. Jelezko, T. Gaebel, I. Popa, A. Gruber, and J. Wrachtrup, Phys. Rev. Lett. **92**, 076401 (2004).
[70] N. Aslam, G. Waldherr, P. Neumann, F. Jelezko, and J. Wrachtrup, New Journal of Physics **15**, 013064 (2013).
[71] S. Meiboom and D. Gill, Review of Scientific Instruments **29**, 688 (1958).
[72] T. H. Taminiau, J. Cramer, T. van der Sar, V. V. Dobrovitski, and R. Hanson, Nat Nano **9**, 171 (2014).
[73] L. Cywiński, R. M. Lutchyn, C. P. Nave, and S. Das Sarma, Phys. Rev. B **77**, 174509 (2008).
[74] R. de Sousa, in *Electron Spin Resonance and Related Phenomena in Low-Dimensional Structures Topics in Applied Physics*, Vol. 115, edited by M. Fanciulli (Top. Appl. Phys., 2009) p. 183.
[75] A. L. McWhorter (Univ Penn Press, 1957).
[76] J. Labaziewicz, Y. Ge, D. R. Leibrandt, S. X. Wang, R. Shewmon, and I. L. Chuang, Phys. Rev. Lett. **101**, 180602 (2008).
[77] J. H. Cole and L. C. L. Hollenberg, Nanotechnology **20**, 495401 (2009).
[78] L. Luan, M. S. Grinolds, S. Hong, P. Maletinsky, R. L. Walsworth, and A. Yacoby, Scientific Reports **5**, 8119 EP (2015).
[79] A. O. Sushkov, I. Lovchinsky, N. Chisholm, R. L. Walsworth, H. Park, and M. D. Lukin, Phys. Rev. Lett. **113**, 197601 (2014).
[80] I. Lovchinsky, A. O. Sushkov, E. Urbach, N. P. de Leon, S. Choi, K. De Greve, R. Evans, R. Gertner, E. Bersin, C. Müller, L. McGuinness, F. Jelezko, R. L. Walsworth, H. Park, and M. D. Lukin, Science **351**, 836 (2016).
[81] M. Kim, H. J. Mamin, M. H. Sherwood, C. T. Rettner, J. Frommer, and D. Rugar, Applied Physics Letters **105**, 042406 (2014).

[82] S. Cui, A. S. Greenspon, K. Ohno, B. A. Myers, A. C. Bleszynski Jayich, D. D. Awschalom, and E. L. Hu, Nano Letters **15**, 2887 (2015).
[83] F. F. de Oliveira, S. A. Momenzadeh, Y. Wang, M. Konuma, M. Markham, A. M. Edmonds, A. Denisenko, and J. Wrachtrup, Applied Physics Letters **107**, 073107 (2015).
[84] S. Cui and E. L. Hu, Applied Physics Letters **103**, 051603 (2013).
[85] K. Ohashi, T. Rosskopf, H. Watanabe, M. Loretz, Y. Tao, R. Hauert, S. Tomizawa, T. Ishikawa, J. Ishi-Hayase, S. Shikata, C. L. Degen, and K. M. Itoh, Nano Letters **13**, 4733 (2013).
[86] C. Osterkamp, J. Lang, J. Scharpf, C. Müller, L. P. McGuinness, T. Diemant, R. J. Behm, B. Naydenov, and F. Jelezko, Applied Physics Letters **106**, 113109 (2015).
[87] L. C. Bassett, F. J. Heremans, C. G. Yale, B. B. Buckley, and D. D. Awschalom, Phys. Rev. Lett. **107**, 266403 (2011).
[88] C. I. Pakes, D. Hoxley, J. R. Rabeau, M. T. Edmonds, R. Kalish, and S. Prawer, Applied Physics Letters **95**, 123108 (2009)
.